

# Preparation, Crystal Structure, and Magnetic Properties of an Oligonuclear Complex with 12 Coupled Spins and an $S = 12$ Ground State

Andrea Caneschi,<sup>1a</sup> Dante Gatteschi,<sup>\*1a</sup> Jean Laugier,<sup>1b</sup> Paul Rey,<sup>\*1b</sup> Roberta Sessoli,<sup>1a</sup> and Claudia Zanchini<sup>1a</sup>

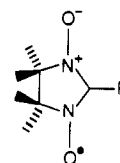
Contribution from the Department of Chemistry, University of Florence, Florence, Italy, and Laboratoire de Chimie, U.A., CNRS 1194, Département de Recherche Fondamentale, Centre d'Etudes Nucleaires, Grenoble, France. Received July 16, 1987

**Abstract:** A novel oligonuclear compound, containing six manganese(II) ions and six nitronyl-nitroxide radicals NITPh (NITPh = 2-phenyl-4,4,5,5-tetramethyl-4,5-dihydro-1H-imidazolyl-1-oxyl 3-oxide),  $[\text{Mn}(\text{hfac})_2\text{NITPh}]_6$ , was synthesized, and its crystal structure, magnetic properties, and EPR spectra are reported. This cyclohexamer crystallizes in the trigonal system, space group  $R\bar{3}$ , with rhombohedral axes  $a = b = c = 21.21(1) \text{ \AA}$ ,  $\alpha = \beta = \gamma = 116.77(2)^\circ$ , and  $Z = 6$ . The structure consists of discrete clusters of six radicals and six  $\text{Mn}(\text{hfac})_2$ , in which each transition-metal ion is in a distorted octahedral environment. Two oxygen atoms belonging to two different nitronyl-nitroxide radical ligands occupy two cis coordination positions around manganese. The temperature dependence of the magnetic susceptibility in the range 300–5 K indicates that the manganese(II) and the radical spins are antiferromagnetically coupled to give an  $S = 12$  ground state. The single-crystal EPR spectra of  $[\text{Mn}(\text{hfac})_2\text{NITPh}]_6$  show both  $M = 1$  and  $M = 2$  transitions. The angular dependence of the line width, which is similar to that of typical one-dimensional materials, is discussed within a model considering the zero-field splitting tensors of the populated spin multiplets.

The magnetic properties of pairs are now reasonably well understood,<sup>2</sup> and data are available also for systems involving infinite arrays of spins.<sup>3,4</sup> In between these limits, considerable work has been performed on clusters of three and four spins, especially because of their relevance to biological problems,<sup>5-9</sup> but much less is known for systems with more than four spins. In fact, efficient general strategies for the preparation of compounds containing a larger number of spins are not easily developed, but recently novel systems assembling eight or more spins have been reported. In one case an organic radical with eight unpaired electrons was synthesized<sup>10</sup> with the purpose of finding the most suitable building blocks to obtain a molecular ferromagnet. Eleven- and eight-nuclear iron complexes were synthesized<sup>11-13</sup> as models for the hydrolytic process of ferritin. The iron complexes were obtained through a hydrolytic process, which did not proceed to yield an infinite array of iron atoms, due to the presence of hydrophobic ligands, which prevented the aggregates to grow too large.

During the course of our systematic attempts to synthesize linear-chain compounds containing transition-metal ions and stable nitronyl-nitroxide radicals,<sup>14-17</sup> we found that by reaction of the

radical 2-phenyl-4,4,5,5-tetramethyl-4,5-dihydro-1H-imidazolyl-1-oxyl 3-oxide (NITPh)



where  $R = \text{phenyl}$ , with  $\text{Mn}(\text{hfac})_2$  ( $\text{hfac} = \text{hexafluoroacetylacetonate}$ ) a 1:1 adduct is formed, which turned out to be the novel oligonuclear species cyclohexakis $[\mu\text{-}1,3\text{-}(2\text{-phenyl-}4,4,5,5\text{-tetramethyl-}4,5\text{-dihydro-}1\text{H-imidazolyl-}1\text{-oxyl } 3\text{-oxide})\text{bis}(\text{hexafluoroacetylacetonate})\text{manganese(II)}]$ ,  $[\text{Mn}(\text{hfac})_2\text{NITPh}]_6$ . To our knowledge, this discrete molecule is the one so far reported containing the highest number of paramagnetic centers, namely 12, i.e. 6 manganese(II) ions and 6 radicals. We report here the X-ray crystal structure, the magnetic properties, and the EPR spectra of  $[\text{Mn}(\text{hfac})_2\text{NITPh}]_6$ .

## Experimental Section

**Synthesis of the Complex.**  $\text{Mn}(\text{hfac})_2 \cdot 2\text{H}_2\text{O}$  was prepared according to the established procedure.<sup>18</sup> The NITPh radical was prepared as previously described.<sup>19,20</sup> A total of 1 mmol of the manganese(II) salt was dissolved in 50 mL of dry boiling *n*-heptane, and a solution of 1.2 mmol of NITPh dissolved in 15 mL of hot dry *n*-heptane was added. The solution was stirred for 10 min, and then it was allowed to cool to room temperature. After 6 h it was filtered to separate the solution from a dense blue oil and allowed to stand at 4 °C.

Dark green well-developed hexagonal prismatic crystals suitable for X-ray determination were collected after 3 days. The compound analyzed satisfactorily for  $[\text{Mn}(\text{hfac})_2\text{NITPh}]_6$ . Anal. Calcd for  $\text{C}_{23}\text{H}_{25}\text{F}_{12}\text{MnN}_2\text{O}_6$ : C, 39.32; H, 2.71; N, 3.99; Mn, 7.82. Found: C, 39.17; H, 2.78; N, 3.84; Mn, 7.63.

(14) Benelli, C.; Caneschi, A.; Gatteschi, D.; Rey, P. In *Organic and Inorganic Low Dimensional Crystalline Materials*; Delhaes, P., Drillon, M., Eds.; Plenum: New York, in press.

(15) Caneschi, A.; Gatteschi, D.; Laugier, J.; Rey, P. In *Organic and Inorganic Low Dimensional Crystalline Materials*; Delhaes, P., Drillon, M., Eds.; Plenum: New York, in press.

(16) Laugier, J.; Rey, P.; Benelli, C.; Gatteschi, D.; Zanchini, C. *J. Am. Chem. Soc.* **1986**, *108*, 6931.

(17) Caneschi, A.; Gatteschi, D.; Zanchini, C.; Rey, P. *J. Chem. Soc., Faraday Trans. 2*, in press.

(18) Cotton, F. A.; Holm, R. H. *J. Am. Chem. Soc.* **1960**, *82*, 2979.

(19) Lamchen, M.; Wittag, T. W. *J. Chem. Soc. C* **1966**, 2300.

(20) Ullman, E. F.; Call, L.; Osiecki, J. H. *J. Org. Chem.* **1970**, *35*, 3623.

(1) (a) University of Florence. (b) Centre d'Etudes Nucleaires.  
 (2) Willett, R. D.; Gatteschi, D.; Kahn, O., Eds. *Magneto-Structural Correlations in Exchange Coupled Systems*; Reidel: Dordrecht, The Netherlands, 1985.  
 (3) Hatfield, W. E.; Estes, W. E.; Marsh, W. E.; Pickens, M. W.; ter Haar, L. w.; Weller, R. In *Extended Linear Chain Compounds*; Miller, J. S., Ed.; Plenum: New York and London, 1983; Vol. 3, p 43.  
 (4) Willett, R. D.; Gaura, R. M.; Landee, C. P. In *Extended Linear Chain Compounds*; Miller, J. S., Ed.; Plenum: New York and London, 1983; Vol. 3, p 143.  
 (5) Girerd, J. J.; Papaefthymiou, G. C.; Watson, A. D.; Gamp, E.; Hagen, K. S.; Edelstein, N.; Frankel, R. B.; Holm, R. H. *J. Am. Chem. Soc.* **1984**, *106*, 5941.  
 (6) Papaefthymiou, G. C.; Girerd, J. J.; Moura, I.; Moura, J. J. G.; Münck, E. *J. Am. Chem. Soc.* **1987**, *109*, 4703.  
 (7) Gloux, J.; Gloux, P.; Lamotte, B.; Ryus, G. *Phys. Rev. Lett.* **1985**, *54*, 599.  
 (8) Laskowski, E. J.; Reynolds, J. G.; Frankel, R. B.; Foner, S.; Papaefthymiou, G. C.; Holm, R. H. *J. Am. Chem. Soc.* **1979**, *101*, 6562.  
 (9) de Paula, J. C.; Brudvig, G. W. *J. Am. Chem. Soc.* **1986**, *108*, 4002.  
 (10) Teki, Y.; Takui, T.; Itoh, K.; Iwamura, H.; Kobayashi, K. *J. Am. Chem. Soc.* **1983**, *105*, 3722.  
 (11) Gorun, S. M.; Lippard, S. J. *Nature (London)* **1986**, *319*, 666.  
 (12) Gorun, S. M.; Papaefthymiou, G. C.; Frankel, R. B.; Lippard, S. J. *J. Am. Chem. Soc.* **1987**, *109*, 3337.  
 (13) Wiegardt, K.; Pohl, K.; Jibril, I.; Hutther, G. *Angew. Chem., Int. Ed. Engl.* **1984**, *23*, 77.

**Table I.** Crystallographic Data and Experimental Parameters for  $[\text{Mn}(\text{hfac})_2\text{NITPh}]_6$ 

formula	$\text{C}_{23}\text{H}_{19}\text{MnN}_2\text{O}_6\text{F}_{12}$
molecular weight	702.3
cryst syst	rhombohedral
space gp	$R\bar{3}$
cell param	$a = b = c = 21.21 (1) \text{ \AA}$ $\alpha = \beta = \gamma = 116.77 (2)^\circ$ $V = 4358.3 \text{ \AA}^3$ $Z = 6$
$d_{\text{calcd}}$	$1.61 \text{ g/cm}^3$
linear abs	$\mu = 0.6 \text{ mm}^{-1}$
cryst size	$0.30 \times 0.20 \times 0.20 \text{ mm}$
temp	$20^\circ \text{C}$
radiatn	
take-off angle	$6^\circ$
wavelength	$0.7107 \text{ \AA}$ (Mo $K\alpha$ )
monochromator	graphite
Bragg angle	$1^\circ < \theta < 25^\circ$
scan	
mode	$\omega$
range	$0.75 + 0.35 \tan \theta$
speed	$0.6\text{--}4^\circ/\text{min}$
detector window	
height	4 mm
width	$2.40 + 3.0 \tan \theta$
test reflns	(4,1,0), (2,7,-7)
measd reflns	$0 < h < 25, -25 < k < 25, -25 < l < 25$
total no.	5517
$F > 2\sigma(F)$	2254
refinement	
$R$	0.064
$R_w$	0.063
weight	$1/\sigma^2$

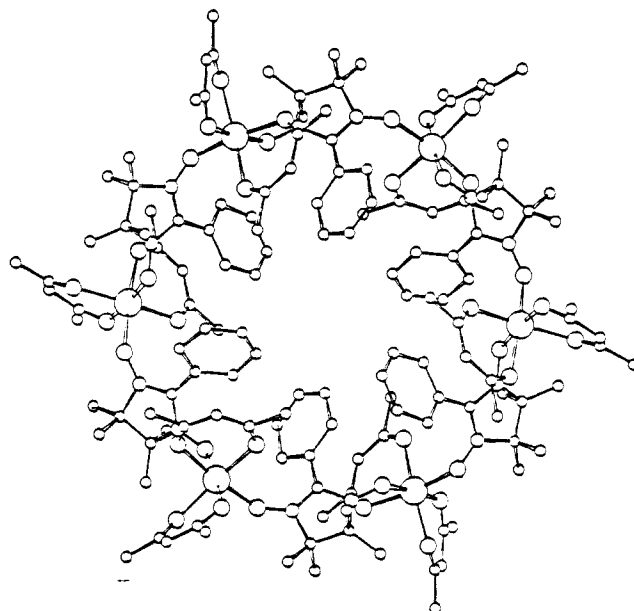
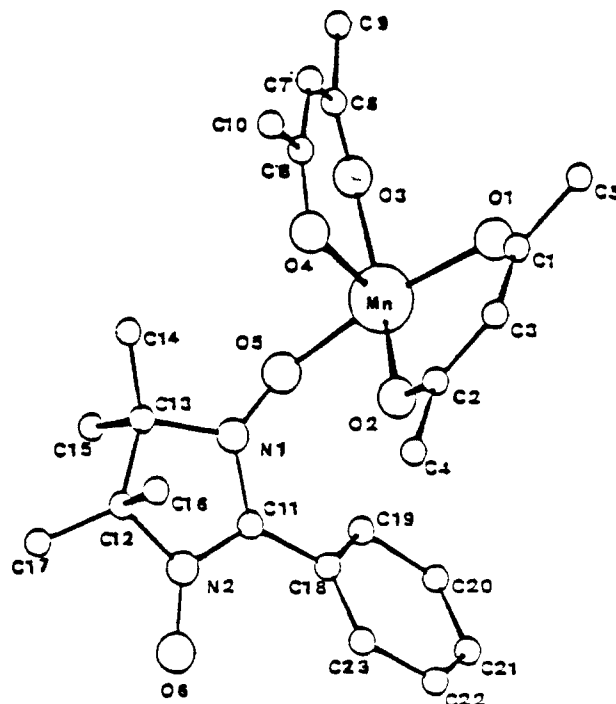
**X-ray Data Collection and Reduction.** Preliminary Weissenberg photographs showed a hexagonal pattern with additional extinctions ( $-h, +k, +l = 3n$ ), which indicated a rhombohedral system. In the rhombohedral cell, 6 molecular units are needed to obtain a density close to 1.5 (value usual for metal nitroxyl species). Therefore, the three space groups  $R\bar{3}$ ,  $R3m$ , and  $R32$  are possible. However, the absence of a symmetry plane and axis is only compatible with the space group  $R\bar{3}$ . The same crystal was mounted on an Enraf-Nonius CAD-4 four-circle diffractometer with Mo  $K\alpha$  radiation. Accurate unit cell parameters were derived from least-squares refinement of the setting angles of 25 reflections and are reported in Table I with the other experimental parameters.

**Structure Solution and Refinement.** The crystal structure was solved by conventional Patterson and Fourier methods using the SHELX-76 package.<sup>21</sup> The phases, provided by the position of the manganese atom, were used for successive difference syntheses that revealed the positions of all the remaining non-hydrogen atoms. Final structure refinements included hydrogen atoms with isotropic thermal parameters in fixed and idealized positions. With 2254 reflections ( $|F_o| > 2\sigma|F_o|$ ), the refinement converged to final  $R$  values of  $R = 0.064$  and  $R_w = 0.063$ . The esd's of the atomic positional parameters as well as the thermal parameters are larger than usual. This is likely due to the rodlike shape of the crystal and the poor quality of the data obtained at high  $\theta$  ( $>20^\circ$ ). However, this poor precision of the parameters does not hamper the chemical meaning of the structure.

Atomic positional parameters are listed in Table II, and relevant bond lengths and angles, in Tables III and IV. Complete listings of anisotropic thermal parameters and observed and calculated structure factors are deposited as supplementary materials (Tables SI–SII).

**Magnetic Susceptibility Measurements.** Magnetic susceptibilities were measured in the temperature range 300–5 K with an SHE superconducting SQUID susceptometer at variable field strengths. Data were corrected for the magnetization of the sample holder and for diamagnetic contributions, which were estimated from Pascal constants.

**Electron Paramagnetic Resonance Measurements.** EPR spectra of  $[\text{Mn}(\text{hfac})_2\text{NITPh}]_6$  were recorded with a Bruker ER200 and a Varian E9 spectrometer operating at X- and Q-band frequencies, respectively. Low-temperature spectra were recorded with an Oxford Instruments ESR9 continuous-flow cryostat. Single crystals of  $[\text{Mn}(\text{hfac})_2\text{NITPh}]_6$

**Figure 1.** View of the cyclic hexanuclear unit of  $[\text{Mn}(\text{hfac})_2\text{NITPh}]_6$ . The fluorine atoms of the hexafluoroacetylacetonate ligands have been omitted for the sake of clarity.**Figure 2.** Asymmetric unit of  $[\text{Mn}(\text{hfac})_2\text{NITPh}]_6$ . The coordination polyhedron of the manganese(II) ion is completed by an oxygen atom, namely O6, belonging to another NITPh ligand.

were oriented with a Philips PW 1100 diffractometer and were found to have largely developed ( $\bar{2}10$ ) and  $2\bar{1}0$ ) faces.

## Results

**Crystal Structure.** The structure consists of discrete clusters of six manganese(II) ions and six radicals, as shown in Figure 1. The six metal ions and the O–N–C–N–O atoms of the six radicals define a 36-membered macrocycle, whose diameter can be estimated as  $14.7 \text{ \AA}$  from the distance of two opposite manganese(II) ions. In Figure 1 the fluorine atoms of the hexafluoroacetylacetonate ligands have been omitted for the sake of clarity. In Figure 2 the asymmetric unit is shown. Each manganese atom is hexacoordinate to four oxygen atoms of two different hfac molecules and two oxygen atoms of two different NITPh radicals. The coordination polyhedron is a distorted

(21) (a) Sheldrick, G. *SHELX 76 System Of Computing Programs*; University of Cambridge: Cambridge, England, 1976. (b) Busing, W. R.; Martin, K. O.; Levy, H. A. *Oak Ridge Natl. Lab., [Rep.] ORNL (U.S) 1971, ORNL-594-32*.

Table II. Positional Parameters ( $\times 10^4$ ) for [Mn(hfac)<sub>2</sub>NITPh]<sub>6</sub>

	x	y	z	B <sub>eq</sub>		x	y	z	B <sub>eq</sub>
Mn	6255 (1)	4461 (1)	-1564 (1)	5.89	C2	7973 (7)	6774 (7)	-512 (7)	5.84
O1	6460 (4)	5676 (4)	-565 (4)	6.61	C3	8097 (8)	7423 (8)	278 (8)	6.05
O2	7247 (4)	5660 (4)	-1376 (4)	5.93	C4	8794 (9)	7447 (8)	-410 (10)	10.88
O3	5825 (4)	3739 (4)	-1170 (4)	6.51	C5	7524 (9)	7553 (9)	1063 (9)	9.27
O4	8108 (5)	5772 (5)	187 (5)	7.65	C6	6485 (9)	4258 (9)	-162 (9)	6.18
O5	5898 (5)	3203 (4)	-2744 (5)	6.86	C7	7745 (10)	5376 (10)	956 (10)	7.96
O6	6766 (4)	3206 (4)	-4387 (4)	6.20	C8	8421 (9)	6016 (9)	992 (9)	7.91
F1	8637 (9)	7783 (11)	-713 (12)	18.62	C9	5830 (9)	3597 (9)	-147 (9)	9.12
F2	9167 (9)	7238 (8)	-565 (10)	19.40	C10	9828 (12)	7234 (13)	2238 (12)	13.07
F3	9907 (7)	8590 (7)	751 (7)	19.10	C11	6085 (8)	3138 (7)	-3767 (8)	4.98
F4	6548 (5)	6993 (5)	626 (5)	12.49	C12	7832 (10)	3818 (11)	-2650 (10)	8.39
F5	8144 (7)	8585 (6)	1586 (7)	16.33	C13	7274 (11)	3415 (12)	-2435 (11)	9.10
F6	8219 (6)	7912 (6)	2020 (6)	14.34	C14	8003 (11)	4054 (12)	-1255 (11)	13.02
F7	10381 (6)	7121 (8)	2261 (7)	20.36	C15	6364 (13)	1982 (14)	-3440 (14)	15.23
F8	10297 (6)	8113 (6)	2546 (6)	18.95	C16	8927 (9)	5296 (11)	-1505 (10)	13.98
F9	10184 (6)	7653 (8)	3171 (6)	21.52	C17	8247 (10)	3497 (11)	-2875 (10)	11.19
F10	4940 (7)	3260 (8)	-602 (8)	16.25	C18	5116 (9)	2804 (8)	-4587 (8)	5.70
F11	5351 (8)	2583 (7)	-796 (8)	17.90	C19	4025 (10)	1949 (9)	-5121 (9)	8.29
F12	6488 (6)	4165 (7)	916 (6)	16.68	C20	3065 (11)	1606 (11)	-5988 (11)	9.91
N1	6408 (6)	3313 (6)	-2940 (7)	5.98	C21	3310 (15)	2155 (16)	-6187 (13)	11.41
N2	6820 (6)	3315 (6)	-3709 (6)	5.56	C22	4355 (15)	2973 (14)	-5649 (12)	10.13
C1	7320 (7)	6786 (7)	171 (7)	5.71	C23	5294 (10)	3306 (10)	-4849 (9)	7.84

Table III. Bond Lengths (Å) for [Mn(hfac)<sub>2</sub>NITPh]<sub>6</sub>

Mn-O1	2.135 (9)	C11-C18	1.452 (24)
Mn-O2	2.136 (9)	C12-C13	1.505 (37)
Mn-O3	2.111 (10)	C12-C16	1.619 (20)
Mn-O4	2.163 (7)	C12-C17	1.446 (37)
Mn-O5	2.101 (10)	C13-C14	1.436 (30)
Mn-O6	2.170 (6)	C13-C15	1.637 (30)
O5-N1	1.289 (20)	C18-C19	1.391 (24)
O6-N2	1.289 (17)	C18-C23	1.394 (31)
O1-C1	1.249 (12)	C19-C20	1.464 (30)
O2-C2	1.262 (12)	C20-C21	1.378 (45)
O3-C6	1.240 (19)	C21-C22	1.303 (37)
O4-C8	1.223 (23)	C22-C23	1.398 (36)
N1-C11	1.336 (24)	F1-C4	1.210 (36)
N1-C13	1.493 (30)	F2-C4	1.161 (32)
N2-C11	1.358 (24)	F3-C4	1.321 (17)
N2-C12	1.492 (23)	F4-C5	1.273 (21)
C1-C3	1.405 (24)	F5-C5	1.273 (21)
C1-C5	1.506 (25)	F5-C5	1.287 (21)
C2-C3	1.405 (24)	F6-C5	1.332 (22)
C2-C4	1.503 (27)	F7-C10	1.283 (35)
C6-C7	1.380 (11)	F8-C10	1.240 (31)
C6-C9	1.490 (30)	F9-C10	1.319 (30)
C7-C8	1.399 (32)	F10-C9	1.236 (25)
C8-C10	1.537 (13)	F11-C9	1.287 (23)
		F12-C9	1.300 (21)

octahedron with a cis coordination of the two radicals. In this respect, the present compound is different from the previously reported bis(nitroxide) adducts of manganese hexafluoroacetylacetonate, Mn(hfac)<sub>2</sub>(TEMPO)<sub>2</sub> (TEMPO = 2,2,6,6-tetramethylpiperidyl-1-oxyl) and Mn(hfac)<sub>2</sub>(PROXYL)<sub>2</sub> (PROXYL = 2,2,5,5-tetramethylpyrrolidyl-1-oxyl), which are trans derivatives.<sup>22</sup> Each NITPh ligand is bound to two different manganese(II) ions.

The average distance of the manganese(II) ion from the oxygen atoms of the hfac ligands compares well with those reported for the TEMPO and PROXYL adducts.<sup>22</sup> The distances of the manganese ions from the oxygen atoms of the radical are markedly different from each other, Mn-O5 being 2.100 (6) Å, while Mn-O6 is 2.170 (5) Å. It must be remarked that Mn-O6 is opposite to Mn-O4, which has the largest distance relative to the hfac ligands. Therefore, the coordination polyhedron around manganese is an elongated octahedron.

The Mn-O-N angles are much less different from each other, Mn-O5-N1 being 132.7 (3)° and Mn-O6-N3 being 129.5 (4)°. Both angles are much smaller than those observed in Mn-

Table IV. Bond Angles (deg) for [Mn(hfac)<sub>2</sub>NITPh]<sub>6</sub>

O1-Mn-O2	85.0 (3)	O3-C6-C9	115.8 (8)
O1-Mn-O3	90.2 (3)	C7-C6-C9	115.3 (17)
O1-Mn-O4	87.6 (3)	C6-C7-C8	118.1 (18)
O1-Mn-O5	171.9 (3)	O4-C8-C7	131.8 (8)
O1-Mn-O6	86.4 (2)	O4-C8-C10	111.0 (18)
O2-Mn-O3	162.2 (1)	C7-C8-C10	107.1 (17)
O2-Mn-O4	81.3 (3)	F10-C9-F11	113.2 (11)
O2-Mn-O5	91.6 (3)	F10-C9-F12	105.3 (19)
O2-Mn-O6	100.8 (3)	F10-C9-C6	115.0 (20)
O3-Mn-O4	81.4 (3)	F11-C9-F12	103.2 (18)
O3-Mn-O5	95.2 (4)	F11-C9-C6	111.7 (19)
O3-Mn-O6	95.9 (3)	F12-C9-C6	117.0 (8)
O4-Mn-O5	99.2 (3)	F7-C10-F8	106.9 (21)
O4-Mn-O6	173.4 (4)	F7-C10-F9	106.7 (21)
O5-Mn-O6	87.0 (3)	F7-C10-C8	111.8 (16)
O5-N1-C11	125.3 (13)	F8-C10-F9	102.8 (16)
O5-N1-C13	122.8 (16)	F8-C10-C8	115.0 (22)
C11-N1-C13	110.9 (17)	F9-C10-C8	112.8 (20)
O6-N2-C11	125.3 (12)	N1-C11-N2	107.3 (13)
O6-N2-C12	121.8 (14)	N1-C11-C18	126.3 (17)
C11-N2-C12	112.5 (15)	N2-C11-C18	126.4 (17)
O1-C1-C3	130.7 (14)	N2-C12-C13	99.5 (15)
O1-C1-C5	114.2 (14)	N2-C12-C16	104.4 (18)
C3-C1-C5	115.1 (11)	N2-C12-C17	112.2 (16)
O2-C2-C3	132.4 (14)	C13-C12-C16	105.4 (16)
O2-C2-C4	108.8 (13)	C13-C12-C17	122.8 (23)
C3-C2-C4	118.8 (11)	C16-C12-C17	110.6 (14)
C1-C3-C2	118.5 (11)	N1-C13-C12	102.5 (20)
F1-C4-F2	112.2 (25)	N1-C13-C14	112.7 (21)
F1-C4-F3	92.6 (13)	N1-C13-C15	103.9 (11)
F1-C4-C2	117.3 (19)	C12-C13-C14	122.8 (13)
F2-C4-F3	93.3 (13)	C12-C13-C15	104.4 (20)
F2-C4-C2	122.9 (19)	C14-C13-C15	108.8 (23)
F3-C4-C2	110.7 (17)	C11-C18-C19	118.1 (18)
F4-C5-F5	108.3 (18)	C11-C18-C23	119.0 (15)
F4-C5-F6	104.6 (17)	C19-C18-C23	122.9 (17)
F4-C5-C1	114.7 (6)	C18-C19-C20	115.1 (20)
F5-C5-F6	102.4 (8)	C19-C20-C21	119.0 (19)
F5-C5-C1	115.1 (18)	C20-C21-C22	124.1 (29)
F6-C5-C1	110.4 (17)	C21-C22-C23	119.9 (30)
O3-C6-C7	128.9 (20)	C18-C23-C22	118.9 (19)

(hfac)<sub>2</sub>(TEMPO)<sub>2</sub> (167.2 (5)°) and in Mn(hfac)<sub>2</sub>(PROXYL)<sub>2</sub> (145.3 (4)°).

The bond distances and angles within the radical moieties compare well with those previously reported from NITPh.<sup>16,23</sup> The dihedral angle between the phenyl ring and the radical plane is 50.5°, larger than that found in other structures of coordinated

(22) Dickman, M. H.; Porter, L. C.; Doedens, R. J. *Inorg. Chem.* 1986, 25, 2595.

(23) Wong, W.; Watkins, S. F. *J. Chem. Soc., Chem. Commun.* 1973, 888.

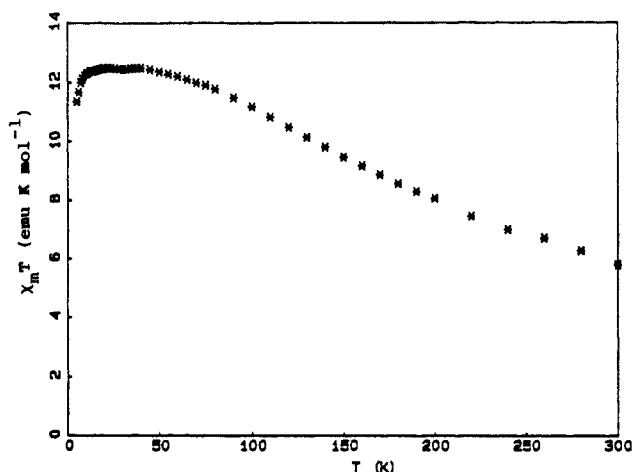


**Figure 3.** Temperature dependence of the experimental magnetic susceptibility of  $[\text{Mn}(\text{hfac})_2\text{NITPh}]_6$ , expressed for the monomeric formula, in the  $\chi T$  vs  $T$  form, obtained at a field of 0.5 T.

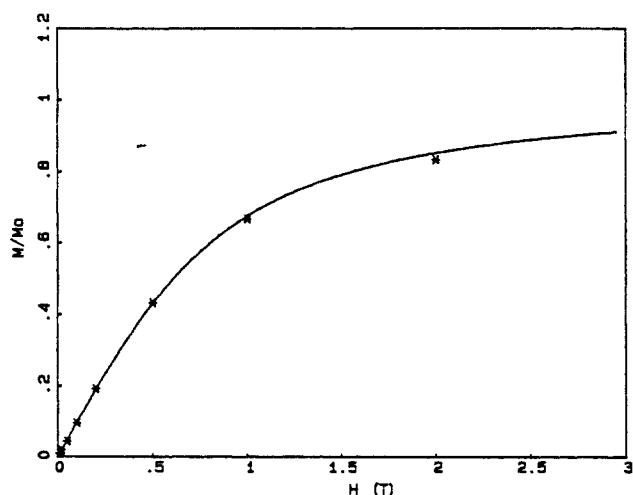


**Figure 4.** Magnetization measurements performed at 6 K for  $[\text{Mn}(\text{hfac})_2\text{NITPh}]_6$  in the form  $M/M_0$  vs  $H$  ( $M_0 = Ng\mu_B S$ ): (\*) experimental values, (—) calculated curve.

NITPh.<sup>16</sup> It is very probable that such a larger dihedral angle is necessary to release steric hindrance around the NO group. The phenyl rings lie inside the 36-membered macrocycle, and close inspection of the structure shows that each of them is almost parallel ( $8^\circ$ ) to one hexafluoroacetylacetonate plane, the distance between the two planes being 3.42 Å. Such a short distance allows interaction<sup>24</sup> between the two  $\pi$ -systems, which probably acts as the driving force for the ring closure and accounts, at least in part, for the stability of the cyclic hexameric structure.

**Magnetic Data.** The temperature dependence of the magnetic susceptibility of  $[\text{Mn}(\text{hfac})_2\text{NITPh}]_6$  in the  $\chi T$  vs  $T$  form is shown in Figure 3. The magnetic susceptibility was calculated for one manganese. The curve, which was obtained at a field of 0.5 T, increases steadily on lowering temperature from 300 to ca. 50 K. Below this limit a plateau corresponding to  $\chi T = 12.5 \text{ emu K mol}^{-1}$  is reached, and below 10 K a small decrease is observed. The room-temperature value,  $5.79 \text{ emu K mol}^{-1}$ , is significantly higher than that expected for uncorrelated manganese and radical spins ( $4.75 \text{ emu K mol}^{-1}$ ).

Magnetization measurements were performed at 6 K. The results are shown in Figure 4: large saturation effects begin to show up above 0.2 T. The curve in Figure 4 was calculated as indicated in the Discussion.

**EPR Spectra.** Single-crystal EPR spectra of  $[\text{Mn}(\text{hfac})_2\text{NITPh}]_6$  were recorded at room temperature at both X-

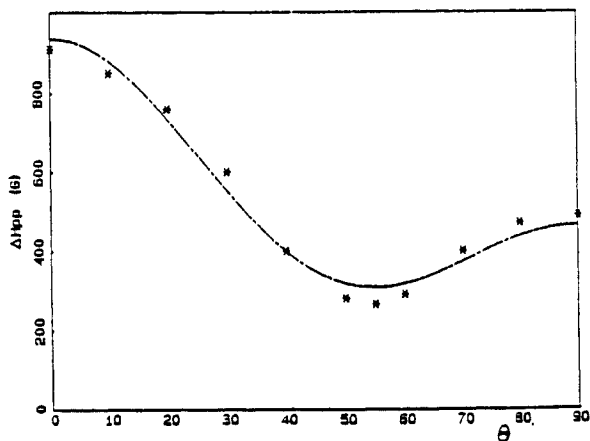


**Figure 5.** Angular dependence of the line width of the main line in a plane containing the hexagonal axis at Q-band frequency at room temperature.  $\theta$  is the angle of the external magnetic field with the hexagonal axis. The solid line is calculated by the equation  $\Delta H_{pp} = a + b(3 \cos^2 \theta - 1)^2$  with  $a = 30.74 \text{ mT}$  and  $b = 15.68 \text{ mT}$ .

and Q-band frequencies. In most field orientations only one band, centered at  $g = 2$ , is observed. Notable exceptions to this are observed when the direction of the static magnetic field makes an angle  $\theta$  of ca.  $55^\circ$  with the hexagonal axis, where one transition at half-field is clearly observed. A reasonable intensity of this transition was found for  $\theta$  ranging from  $35^\circ$  to  $65^\circ$ . The resonance field is independent of the crystal orientation. The line width is practically the same at both X- and Q-band frequencies. The width of the main line is largely anisotropic in the planes containing the hexagonal axis, as shown in Figure 5. The maximum peak-to-peak line width,  $0.095 \text{ T}$ , is observed parallel to the hexagonal axis, and a lower maximum is observed orthogonal to that,  $0.051 \text{ T}$ , while the minimum,  $0.028 \text{ T}$ , is observed at the magic angle. The line width is within error isotropic in the plane orthogonal to the hexagonal axis. The angular dependence of the line width is reminiscent of the angular behavior of typical one-dimensional materials,<sup>25-27</sup> and indeed it can be nicely reproduced with the equation  $\Delta H_{pp} = a + b(3 \cos^2 \theta - 1)^n$  where  $a$  and  $b$  are determined by a least-squares procedure. The best fit values, calculated for the room-temperature Q-band spectra, are  $a = 30.74 \text{ mT}$  and  $b = 15.68 \text{ mT}$  for  $n = 2$  with the agreement factor  $R = 0.990$ .

The line shape was analyzed with the standard procedure,<sup>28,29</sup> and it was found to be essentially Gaussian in all the angular settings.

In the X-band spectra recorded at 4.2 K, the lines become much broader than at room temperature; for instance, with the static magnetic field parallel to the hexagonal axis, a broad signal with  $\Delta H_{pp} = 0.34 \text{ T}$  is observed. In several field positions there is evidence for more than one transition, although very ill-defined. The lines are reasonably narrow at the magic angle where an absorption at  $g = 2$  is observed, with  $\Delta H_{pp} = 0.036 \text{ T}$ . At this angular setting the half-field transition is also observed.

## Discussion

The temperature dependence of  $\chi T$  shows that the manganese(II) and radical spins are coupled. The plateau reached at low temperature indicates that the ground state has a definite spin value and is well separated from the excited states. In the simplest approach we may consider only nearest-neighbor interactions, and neglecting the small differences in the manganese-radical bond

(25) Richards, P. M. In *Local Properties of Phase Transition*; Muller, K. A., Ed.; North-Holland: Amsterdam, The Netherlands, 1975; p 539.

(26) Kokoszka, G. F. In *ESR of Low Dimensional Systems, Low Dimensional Cooperative Phenomena*; Keller, H. J., Ed.; Plenum: New York, 1975; p 171.

(27) Drumheller, J. E. *Magn. Reson. Rev.* **1982**, *7*, 123.

(28) Bartkowski, R. R.; Morosin, B. *Phys. Rev. B* **1972**, *6*, 4209.

(29) Bartkowski, R. R.; Hennessy, M. J.; Morosin, B.; Richards, P. M. *Solid State Commun.* **1972**, *11*, 405.

(24) Prinzbach, H.; Sedelmeier, G.; Kruger, C.; Goddard, R.; Martin, H. D.; Gleiter, R. *Angew. Chem., Int. Ed. Engl.* **1978**, *17*, 271.

distances, we assume that one constant describes the coupling. In other terms we use for the system the following Hamiltonian

$$\mathcal{H} = J \sum_{i=1}^6 S_{\text{Mn}_i}(S_{r_i} + S_{r_{i-1}})$$

with the cyclic condition that  $S_{r_6} = S_{r_1}$ . The overall degeneracy of the spin states for this system is  $2^6 \times 6^6 = 2985984$ . When the states are classified by the total spin operator  $S = \sum_i S_i$ , the levels are organized in multiplets, with  $S$  ranging from 0 to 18 and multiplicities ranging from 1 to 36 120. It is apparent that even in this way the calculation of the energies of the states is a formidable task. A further reduction of the dimensions of the matrices might be achieved by using the symmetry of the real space,<sup>30</sup> which should afford a reduction of the order of the matrices by 5. Even when these techniques are used, it has been possible, to our knowledge, only to treat the "simple" problem of five pairs of  $S_1 = 1/2$  and  $S_2 = 1$  spins, while for pairs of  $S_1 = 1/2$  and  $S_2 = 5/2$  spins, such as the present one, only clusters of three pairs have been treated.<sup>31-34</sup>

However, even if the energy levels of six pairs must remain largely undetermined, it is possible to give an estimate of the coupling, by approximate arguments.

In the limit of strong ferromagnetic coupling, the ground state has  $S = 18$ , with an expected  $\chi T$  value of 28.5 emu mol<sup>-1</sup> K for  $g = 2.00$ . For strong antiferromagnetic coupling, all the manganese spins are up and the radical ones are down, yielding a ground state  $S = 12$ , with an expected  $\chi T = 13$  emu K mol<sup>-1</sup>. Therefore, these two states should be easily discriminated at low temperature. The low-temperature limit of  $\chi T$  observed for [Mn(hfac)<sub>2</sub>NITPh]<sub>6</sub> is very close to the latter value, suggesting that the ground state is indeed  $S = 12$ . This is confirmed by the magnetization data of Figure 4, which can be fitted quite well with a Brillouin curve calculated for  $S = 12$ . The fact that the observed  $\chi T$  value is slightly lower than the expected one is mainly due to saturation effects.

Therefore, we can conclude that the ground state of [Mn(hfac)<sub>2</sub>NITPh]<sub>6</sub> is  $S = 12$ . This result is in line with the findings in ferrimagnetic alternating heterometallic chains containing copper(II) and manganese(II) ions, in which large moments are generated by the uncompensation of  $S = 1/2$  and  $S = 5/2$  spins antiferromagnetically coupled.<sup>35,36</sup> The interpretation of the magnetic properties of these chains has shown<sup>35-37</sup> that a minimum in the  $\chi T$  vs  $T$  curve must be observed at a temperature  $T_{\text{min}} \approx 2.5J$ , if the coupling constant is expressed in kelvin. The expected value of  $\chi T$  at the minimum is around 4.0 emu K mol<sup>-1</sup>. This behavior is not peculiar of chains, but rather it is determined by the antiferromagnetic interaction between different spins. In fact, in this case, the highest energy state is the one of largest spin multiplicity,  $S = 18$  for our cluster, and decreasing temperature determines a selective depopulation of this state, with a neat decrease in  $\chi T$ . However, the lowest energy state is not  $S = 0$ , and a further decrease in temperature selectively populates the ground state, which has a relatively high multiplicity,  $S = 12$  for our cluster. Therefore, the curve of  $\chi T$  goes through a minimum when the number of pairs of different spins is larger than one.

We do not observe any minimum in our curve, but rather  $\chi T$  steadily increases on raising  $T$ . This might be attributed to ferromagnetic coupling, but in this case, the low-temperature  $\chi T$

limit value should be much larger. Therefore, we must conclude that the coupling between manganese(II) and NITPh is antiferromagnetic. Since the  $\chi T$  value at room temperature is already higher than that expected for the minimum, we must conclude that  $T_{\text{min}} > 300$  K or that  $J > 83$  cm<sup>-1</sup>. This result compares well with the reported values of bis(nitroxide) adducts of Mn(hfac)<sub>2</sub>, in which  $J$  was found to be 158 and 210 cm<sup>-1</sup> for the TEMPO and PROXYL ligands, respectively.<sup>22</sup> This result is interesting because it shows the possibility of obtaining ferrimagnetic chains with manganese(II) and NITR radicals with coupling constants much larger than those so far observed in copper(II)-manganese(II) chains.

The magnetic properties of [Mn(hfac)<sub>2</sub>NITPh]<sub>6</sub> are intermediate between those of pairs and of chains; therefore, it is interesting to see whether similar behavior is observed in the EPR spectra. Indeed at first sight the EPR spectra of [Mn(hfac)<sub>2</sub>NITPh]<sub>6</sub> are similar to those expected for typical linear-chain compounds with the  $(3 \cos^2 \theta - 1)^n$  dependence of the line width. However, the line shape for a chain is expected to be Lorentzian or the Fourier transform of  $\exp(-t^{3/2})$ ,<sup>25</sup> while we found it Gaussian. In particular the line is Gaussian also at the magic angle, where a Lorentzian shape is expected for the chain.

We interpret the observed angular behavior of the EPR line width of [Mn(hfac)<sub>2</sub>NITPh]<sub>6</sub> within a model developed for iron clusters.<sup>38</sup>

Each  $S$  level of the cluster will be in general split in zero field by the effect of the zero-field splitting tensor of the individual manganese(II) ions and by the anisotropic spin-spin tensor. Although each tensor is not generally axial, their sum over the cluster must be axial due to the symmetry present in the crystal. Since the number of populated levels is so large, there will be many allowed transitions that add up to a Gaussian line shape. The angular dependence of the line width, which is proportional to the second moment, is easily calculated to be of the  $(3 \cos^2 \theta - 1)^2$  type. Also, the presence of half-field transitions is as expected, with maximum intensities at the angular settings in which the nonsecular terms of the zero-field splitting Hamiltonian are close to a maximum.

A second broadening mechanism may be given by the intermolecular dipolar interactions. Since the lattice is hexagonal, the dipolar second moment is expected to be axial, again with a  $(3 \cos^2 \theta - 1)^2$  dependence. Therefore, the two mechanisms occur for the same result, and indeed the experimental points can be satisfactorily fit to this law, as shown in Figure 5. Since the intermolecular distances between the clusters are long, the second mechanism is expected to be less effective than the first in broadening the lines.

## Conclusions

[Mn(hfac)<sub>2</sub>NITMe]<sub>6</sub> is a crown molecule comprising 12 spins, which are antiferromagnetically coupled to give an  $S = 12$  ground state. To our knowledge, this is the highest value so far reported for a discrete molecule. It is interesting to note that, despite the large  $S$  value, the compound behaves as a paramagnet down to 5 K. It seems therefore that using big spins<sup>39-41</sup> is not sufficient to determine large deviations from the paramagnetic behavior.

**Registry No.** [Mn(hfac)<sub>2</sub>NITPh]<sub>6</sub>, 113378-51-1; Mn(hfac)<sub>2</sub>·2H<sub>2</sub>O, 19648-86-3.

**Supplementary Material Available:** Tables of anisotropic thermal parameters for the non-hydrogen atoms for [Mn(hfac)<sub>2</sub>NITPh]<sub>6</sub> and magnetic data in the range 5–300 K (3 pages); tables of observed and calculated structure factors (11 pages). Ordering information is given on any current masthead page.

(30) Georges, R.; Drillon, M. *Phys. Rev. B* **1982**, *26*, 3882.  
 (31) Verdaguier, M.; Gleize, A.; Renard, J. P.; Seiden, J. *Phys. Rev. B* **1984**, *29*, 5144.  
 (32) Drillon, M.; Coronado, E.; Beltran, D.; Georges, R. *J. Appl. Phys.* **1984**, *57*, 3353.  
 (33) Verdaguier, M.; Julve, M.; Michalowicz, A.; Kahn, O. *Inorg. Chem.* **1983**, *22*, 2624.  
 (34) Drillon, M.; Coronado, E.; Beltran, D.; Curely, J.; Georges, R.; Nugterer, P. R.; de Jongh, L. J.; Genicon, J. L. *J. Magn. Mater.* **1986**, *54-57*, 1507.  
 (35) Pei, Y.; Verdaguier, M.; Kahn, O.; Sletten, J.; Renard, J. P. *Inorg. Chem.* **1987**, *26*, 138.  
 (36) Kahn, O. *Struct. Bonding (Berlin)*, in press.  
 (37) Seiden, J. *J. Phys. Lett.* **1983**, *44*, L947.

(38) Korteweg, G. A.; van Reijen, L. L. *J. Magn. Reson.* **1981**, *44*, 159.  
 (39) Pei, Y.; Journoux, Y.; Kahn, O.; Dei, A.; Gatteschi, D. *J. Chem. Soc., Chem. Commun.* **1986**, 1300.  
 (40) Bencini, A.; Benelli, C.; Caneschi, A.; Dei, A.; Gatteschi, D. *Inorg. Chem.* **1986**, *25*, 572.  
 (41) Bencini, A.; Benelli, C.; Caneschi, A.; Carlin, R. L.; Dei, A.; Gatteschi, D. *J. Am. Chem. Soc.* **1985**, *107*, 8128.